Materials Transactions, Vol. 48, No. 11 (2007) pp. 3024 to 3027

RAPID PUBLICATION

FeSiBP Bulk Metallic Glasses with Unusual Combination of High Magnetization and High Glass-Forming Ability

Akihiro Makino[1], Takeshi Kubota[1], Chuntao Chang[1], Masahiro Makabe[1,*] and Akihisa Inoue[2]

[1]*Institute for Materials research, Tohoku University, Sendai 980-8577, Japan*
[2]*Tohoku University, Sendai 980-8577, Japan*

Among many kinds of bulk metallic glasses (BMGs), Fe-based BMGs with good magnetic properties, high strength and low materials cost should have great potential for wide variety of applications. However, the glass-forming metal elements such as Al, Ga, Nb, Mo, Y and so forth in the Fe-based BMGs significantly decrease saturation magnetization (J_s) which is a essential property as soft magnetic materials and also increase the material cost.

The coexistence of high Fe content and high glass-forming ability (GFA) has been earnestly desired from academia to industry. We report a novel $Fe_{76}Si_9B_{10}P_5$ (at%) bulk metallic glass with unusual combination of high J_s of 1.51 T due to high Fe content and high GFA leading to a glassy rod with a diameter of 2.5 mm despite not-containing any glass-forming metal elements. This alloy composed of familiar and low-priced elements, also exhibiting very excellent magnetic softness and rather high strength, has a great advantage for engineering and industry, and thus should make a contribution to conservation of earth resources and environment through energy saving.
[doi:10.2320/matertrans.MRP2007198]

(Received August 10, 2007; Accepted September 7, 2007; Published October 18, 2007)

Keywords: *soft magnetic material, Metallic glass, high magnetization, grass-forming ability*

1. Introduction

Fe-metalloid (B, C, Si, P)-based ferromagnetic bulk metallic glasses (BMGs) containing glass-forming metal elements such as Al, Ga, Nb, Mo, Y and so forth have been developed.[1–6] These alloys have a GFA leading to the formation of BMG rods with diameters of mm-order prepared by Cu-mold casting with much lower cooling rates than that of melt-spinning used for the production of the Fe-metalloid-based amorphous alloy ribbons with a thickness of less than about 50 μm without glass transition. The development of BMGs overcame the great disadvantage of the melt-spun amorphous ribbons. However, the glass-forming metal elements in BMGs result in a remarkable decrease in saturation magnetization (J_s) from 1.5–1.6 T of the representative Fe-Si-B amorphous alloys widely utilized by industries[7] to less than about 1.3 T. The magnetic elements such as Co and Ni also have some beneficial effects on the GFA in most cases,[8,9] however, the addition of these elements to Fe-based BMGs significantly decreases J_s in the same manner as the glass-forming elements; the substitution of Co for Fe at 50 at% in $(Fe_{0.75}Si_{0.10}B_{0.15})_{96}Nb_4$ significantly increases the critical rod-size of 1.5 mm to 5 mm in diameter, which is the largest size among the soft magnetic BMGs produced by Cu-mold casting, however, rapidly decreases to 1.1 T.[8] The low J_s of the BMGs is a great disadvantage as soft magnetic materials. In addition, these metal elements are rare and expensive, and Al, Nb, Mo and Y also decrease the productivity due to their easy oxidation. It should be, thus, better to avoid the use of these metal elements for high J_s as well as conservation of earth resources and low material cost. Therefore, the development of Fe-based BMGs without any metal elements other than Fe and with relatively high Fe content have been desired for the last one decade, however, has been left unsolved matter over many years. We report a novel $Fe_{76}Si_9B_{10}P_5$ bulk metallic glass with unusual combination of high J_s of 1.51 T due to high Fe content and high GFA leading to a glassy rod with a diameter of 2.5 mm despite not-containing any glass-forming metal elements.

2. Experimental

Fe-Si-B-(P) ingots were prepared by induction melting the mixture of pure metals of Fe (99.98 mass%), pre-melted Fe-P (99.9 mass%), and pure metalloid of crystal B (99.5 mass%) and Si (99.999 mass%) in an argon atmosphere. The alloy compositions represent nominal atomic percent. Amorphous or glassy alloys were produced in a ribbon form by the single roller melt-spinning method and in rod forms by the Cu-mold casting method. The as-spun and as-cast structures were examined by X-ray diffraction (XRD). The glass transition temperature (T_g) and crystallization temperature (T_x) were estimated by a differential scanning calorimetry (DSC) at a heating rate of 0.67 K/s and the liquidus temperature (T_l) was also estimated by a thermogravimetry differential thermal analyzer at a cooling rate of 0.17 K/s. The density (ρ) was measured by the Archimedean method using a pycnometer with Helium gas at 298 K. Cross section of bulk rod with 2.5 mm in diameter was etched for 30 s at room temperature in a solution of 1% hydrofluoric acid and 99% distilled water, and was observed by an optical microscopy. J_s was measured under an applied field of 800 kA/m with a vibrating sample magnetometer. The coercivity (H_c) was measured under a field of 1 kA/m with a DC B-H loop tracer. The specimens for coercivity measurement were heated under a vacuum atmosphere of less than 2×10^{-4} Pa at a heating rate of 0.67 K/s and isothermal annealed at prescribed temperature for 0.6 or 7.2 ks, and then cooled to 295 K by the furnace cooling. Mechanical properties of Young's modulus, compressive fracture strength, elastic strain, and

*Graduate Student, Tohoku University. Present address: Makabe R&D Co. ltd., Sendai 983-0036, Japan

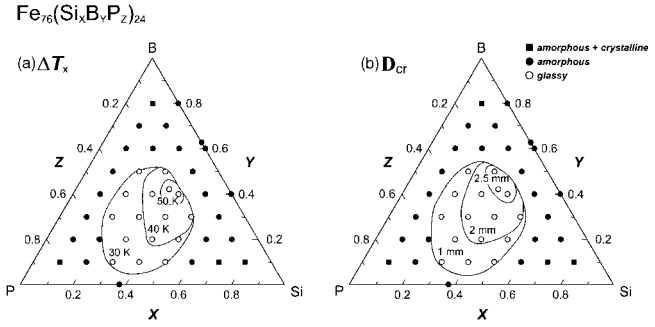

Fig. 1 The compositional dependence of as-quenched structure, supercooled liquid region (ΔT_x) for melt-spun alloys (a), and the critical rod-diameter (D_{cr}) produced by Cu-mold casting in $Fe_{76}(Si_xB_yP_z)_{24}$ ($x+y+z=1$) alloy system.

fracture strain were measured with an Instron testing machine. The specimen dimension was 1.5 mm in diameter and 3 mm in length, and the strain rate was $5.0 \times 10^{-4}\,s^{-1}$. The characteristics of the fractured surface was studied by scanning electron microscopy (SEM). All the measurements were carried out at room temperature.

3. Results and Discussion

Figure 1 shows (a) the compositional dependence of as-quenched structure and supercooled liquid region (ΔT_x) for melt-spun alloys and (b) the critical rod-diameter produced by Cu-mold casting in $Fe_{76}(Si_xB_yP_z)_{24}$ ($x+y+z=1$) alloy system, respectively. The number in Fig. 1(a) represents the temperature interval (ΔT_x), known to be one of the indicators for GFA,[10] between T_g and T_x. In Fig. 1(a) and 1(b), "glassy" and "amorphous" alloys are distinguished by the presence of glass transition. An amorphous phase was observed in a wide compositional range except higher Si, B and P contents than around 8%. Obvious glass transition was observed at the limited quaternary compositions in the amorphous-forming range and the large ΔT_x of over 40 K is observed in the range of $x = 0.3$–0.5, $y = 0.2$–0.5 and $z = 0.2$–0.4. The largest ΔT_x is 52 K for $Fe_{76}Si_{9.6}B_{9.6}P_{4.8}$ and $Fe_{76}Si_9B_{10}P_5$. The rod with a diameter of 2.5 mm was obtained for the above mentioned alloys and $Fe_{76}Si_{7.2}B_{12}P_{4.8}$ alloy, as shown in Fig. 1(b). Comparing Fig. 1(a) and Fig. 1(b), it can be noted that critical diameter (D_{cr}) coincides with ΔT_x.

Figure 2 shows (a) the optical micrograph and (b) the XRD pattern taken from the cross section of the as-cast $Fe_{76}Si_9B_{10}P_5$ rod with a diameter of 2.5 mm. The XRD pattern reveals only typical halos, and no peaks corresponding to crystalline phases are visible. It is thus to be noticed that a single glassy phase is formed in the diameter range up to 2.5 mm.

It is important in applications as engineering materials to clarify the magnetic and mechanical properties of the Fe-metalloids BMGs. The H_c of $Fe_{76}Si_9B_{10}P_5$ glassy alloy with ΔT_x of 52 K and $Fe_{76}Si_9B_{15}$ amorphous alloy without glass transition as a function of annealing temperature is shown in Fig. 3. The extremely low H_c of 0.8 A/m was obtained for 0.6 ks at 748 K for the glassy alloy. The H_c of the $Fe_{76}Si_9B_{15}$ amorphous alloy reaches a minimum value of 8.0 A/m at

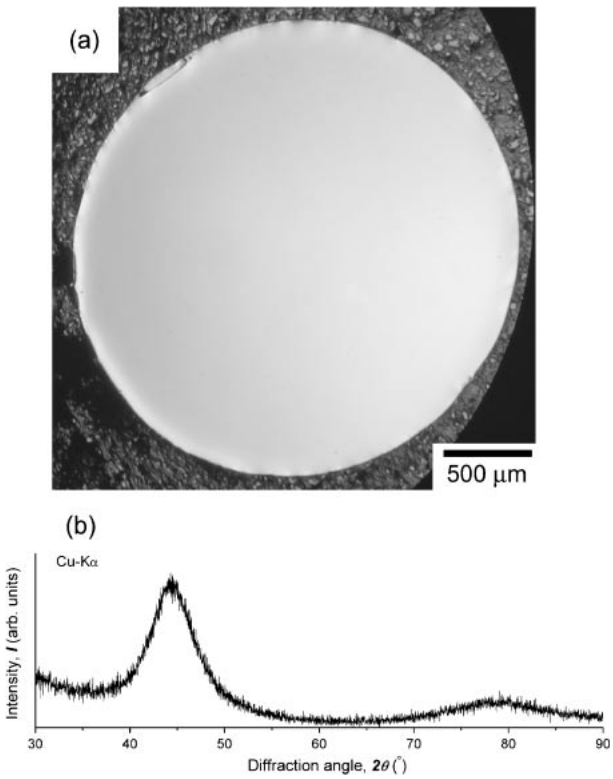

Fig. 2 The optical micrograph (a) and the X-ray diffraction pattern (b) taken from the cross section of the as-cast $Fe_{76}Si_9B_{10}P_5$ rod with a diameter of 2.5 mm.

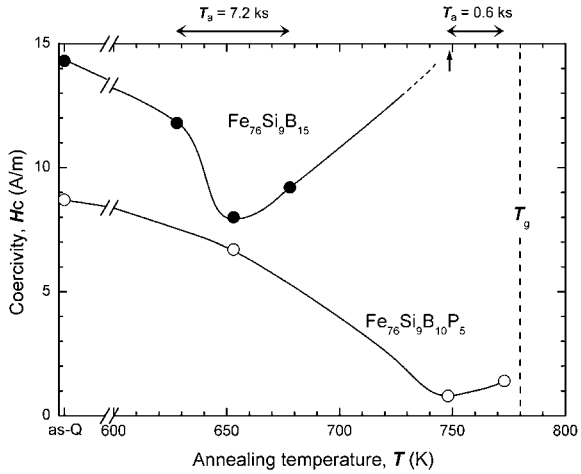

Fig. 3 The coercivity (H_c) of $Fe_{76}Si_9B_{10}P_5$ glassy alloy and $Fe_{76}Si_9B_{15}$ amorphous alloy as a function of annealing temperature.

653 K and rapidly increases with increasing annealing temperature above 653 K, even though an amorphous structure should remain in the temperature range, which is considerably lower than the crystallization temperature of 841 K. On the other hands, the H_c of the $Fe_{76}Si_9B_{10}P_5$ glassy alloy reaches a minimum value of 0.8 A/m at 748 K, 10 times smaller than the minimum H_c of 8.0 A/m for the amorphous alloy, and then slightly increases to 1.4 A/m at 773 K just below the glass transition temperature of 780 K. The ρ in as-quenched state was 7111 kg/m^3 for the $Fe_{76}Si_9B_{15}$ amorphous alloy and 7054 kg/m^3 for the glassy alloy. The ρ of

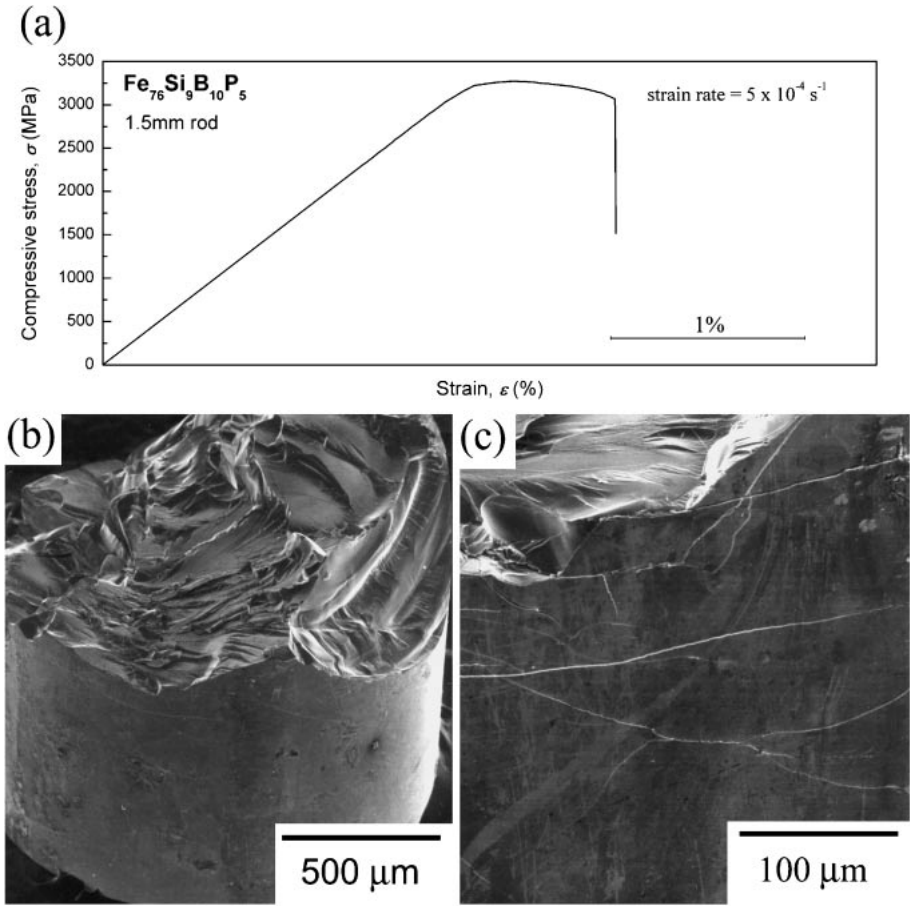

Fig. 4 The compressive stress-strain curve (a), the SEM micrograph revealing the compressive fracture surface (b) and shear bands on the specimen surface (c) of the as-cast $Fe_{76}Si_9B_{10}P_5$ BMG with a diameter of 1.5 mm.

the glassy alloy significantly increases from 7054 kg/m^3 to 7207 kg/m^3 by 2.17% upon the optimum annealing at 748 K. This change is considered to originate from the glass transition from the as-quenched amorphous phase with some inhomogeneity to a glassy phase with a higher degree of atomic density of dense random packed structure. On the contrary, the ρ of the amorphous alloy little changes by 0.22% with annealing because of lack of glass transition. Considering the minimum values of H_c and the annealed structure for the alloys, as described above, the extremely low H_c of 0.8 A/m for the glassy alloy can be explained as due to the dense packed glassy structure. Taking account of the difference in the optimum annealing temperature for H_c, 748 K for the glassy alloy and 653 K for the amorphous alloy, we can see that the $Fe_{76}Si_9B_{10}P_5$ glassy alloy exhibits the higher thermal stability of magnetic softness, which should indicate the higher stability of the glassy phase than the amorphous phase.[11,12)]

Figure 4 shows the compressive stress-strain curve (a), and SEM micrographs revealing the compressive fracture surface (b) and shear bands on the specimen surface (c) of the $Fe_{76}Si_9B_{10}P_5$ BMG with a diameter of 1.5 mm, respectively. It can be seen that the specimen shows an initial elastic deformation behavior with an elastic strain of 1.9%, then begins to yield at about 3.3 GPa, followed by some plastic deformation of 0.7% before fracture. The yield stress is similar to the Fe-based BMGs with the glass-forming elements.[13,14)] The measured Young modulus is 175 GPa. SEM observations show that the fracture under compression occurs in a shear mode. On the specimen surfaces, it is noted that many localized shear bands near the fracture plane were observed, as shown in Fig. 4(c). The shear bands have a relatively high density near the fracture plane. The activation of the shear bands should be a direct evidence for the compressive plasticity of the $Fe_{76}Si_9B_{10}P_5$ BMG.

Table 1 summarizes T_g, T_x, D_{cr}, ΔT_x, T_g/T_l, γ and magnetic properties (J_s, H_c) for the $Fe_{76}Si_9B_{10}P_5$ BMG and the typical Fe-based ferromagnetic BMGs previously reported.[1,2,6,15–18)] Here, ΔT_x, T_g/T_l[19)] and γ ($= T_x/(T_g + T_l)$)[20)] are adopted as the parameters, and the larger all the parameters, the higher is the GFA. The $Fe_{76}Si_9B_{10}P_5$ BMG has the relatively high ΔT_x of 52 K, comparable to the other BMGs, and higher T_g/T_l of 0.62 and γ of 0.41 than those of the other Fe-based BMGs, which are probably one of the reasons for the high GFA of the $Fe_{76}Si_9B_{10}P_5$ BMG leading to the 2.5 mm-diameter specimen.

The $Fe_{76}Si_9B_{10}P_5$ BMG exhibits the highest J_s of 1.51 T among the previously reported Fe-based BMGs due to the high Fe content of 76% and without any metal elements except Fe as well as high GFA leading to the 2.5 mm-diameter specimen.

The P-added Fe-based amorphous and glassy alloys have been investigated for four decades ago.[21–25)] $Fe_{80}P_{13}C_7$[25)] alloys for ternary alloy and Fe-P-B-Si alloy system[2)] for

Table 1 The glass transition temperature (T_g), the crystallization temperature (T_x), the critical diameter (D_{cr}), the parameters (ΔT_x, T_g/T_l and γ), and magnetic properties (J_s, H_c) for the $Fe_{76}Si_9B_{10}P_5$ and the typical Fe-based ferromagnetic BMGs previously reported.

composition	T_g (K)	T_x (K)	ΔT_x (K)	T_g/T_l	γ	J_s (T)	Hc (A/m)	D_{cr} (mm)
$Fe_{76}Si_9B_{10}P_5$	780	832	52	0.62	0.41	1.51	0.8	2.5
$(Fe_{0.75}Si_{0.1}B_{0.15})_{96}Nb_4$	835	885	50	0.61	0.40	1.40	2.9	1.5
$Fe_{74}Al_4Ga_2P_{12}B_4Si_4$	733	782	49	—	—	1.14	6.4	—
$Fe_{73}Al_5Ga_2P_{11}C_5B_4$	732	785	53	—	—	1.29	6.3	1
$Fe_{72}Al_5Ga_2P_{10}C_6B_4Si_1$	732	785	53	—	—	1.14	2.8	2
$Fe_{76}Mo_2Ga_2P_{10}C_4B_4Si_2$	736	788	52	0.59	0.40	1.32	2.9	2
$Fe_{30}Co_{30}Ni_{15}Si_8B_{17}$	780	834	54	—	—	0.92	3.4	1.2
$Fe_{74}Nb_6Y_3B_{17}$	831	789	48	—	—	0.81	15	2

quaternary alloy exhibit the glass transition were reported. However, bulk glassy rod specimen with over 0.5 mm of a diameter have been not yet found, even though ΔT_x of 36 K was obtained for $Fe_{80}P_{12}B_4Si_4$.[2)] Therefore, we can say that this discovery is the first achievement for simultaneous realization of high J_s and high GFA in Fe-based BMGs. In addition, the BMG is composed of 89.17 mass%Fe and small amounts of metalloid elements of Si, B and P. The elements, Fe, Si and P, are the constituent elements in pig-iron produced by the reduction of iron ores typically in a blast furnace. The low-priced Fe-Si and Fe-P ferroalloys are in mass production, thus, there is no restriction in available raw materials. Therefore, the FeSiBP alloy offers great advantages of much lower material cost for engineering and industry, which should make a contribution to conservation of earth resources and environment, and should improve energy saving due to the excellent magnetic softness.

4. Conclusions

(1) The large ΔT_x of over 40 K is observed in the range of $x = 0.3$–0.5, $y = 0.2$–0.5 and $z = 0.2$–0.4 for $Fe_{76}(Si_xB_yP_z)_{24}$ $(x + y + z = 1)$ alloy system. The largest ΔT_x is 52 K for $Fe_{76}Si_{9.6}B_{9.6}P_{4.8}$ and $Fe_{76}Si_9B_{10}P_5$.
(2) $Fe_{76}Si_{9.6}B_{9.6}P_{4.8}$, $Fe_{76}Si_9B_{10}P_5$ and $Fe_{76}Si_{7.2}B_{12}P_{4.8}$ alloys have high GFA leading to a glassy rod with a diameter of 2.5 mm despite not-containing any glass-forming metal elements.
(3) The higher J_s of 1.51 T than those of the previously reported Fe-based BMGs was obtained for $Fe_{76}Si_9B_{10}P_5$ alloy due to the high Fe content of 76% and without any metal elements except Fe.
(4) The extremely low H_c of 0.8 A/m and the high strength of 3.3 GPa and the plastic strain to final failure of 0.7% were obtained for $Fe_{76}Si_9B_{10}P_5$.

Acknowledgements

This work was supported by a Grant-in-Aid for Scientific Research on Priority Areas, "Materials Science of Bulk Metallic Glasses", from the Ministry of Education, Science, Sports and Culture of Japan.

REFERENCES

1) A. Inoue and B. L. Shen: Mater. Sci. Eng. **A375–377** (2004) 302–306.
2) A. Inoue and R. E. Park: Mater. Trans. JIM **37** (1996) 1715–1721.
3) T. Mizushima, K. Ikarashi, A. Makino and A. Inoue: IEEE Trans. Mag. **35** (1999) 3361–3363.
4) H. Koshiba, A. Inoue and A. Makino: J. Appl. Phys. **85** (1999) 5136–5138.
5) A. Makino, A. Inoue and T. Mizushima: Mater. Trans. JIM **41** (2000) 1471–1477.
6) B. L. Shen, M. Akiba and A. Inoue: Phys. Rev. B **73** (2006) 104204-1–104204-6.
7) Metglas®, http://www.metglas.com/
8) A. Inoue, B. L. Shen and C. T. Chang: Acta Mater. **52** (2004) 4093–4099.
9) C. T. Chang, B. L. Shen and A. Inoue: Appl. Phys. Lett. **89** (2006) 051912-1–051912-3.
10) P. R. Okamoto, N. Q. Lam and L. E. Rein: in *solid state physics* **52**, ed. by H. Ehrenreich and F. Spaepen, (Academic Press, San Diego, 1999) pp. 2–133.
11) T. Bitoh, A. Makino and A. Inoue: Mater. Trans. **44** (2003) 2020–2024.
12) T. Bitoh, A. Makino and A. Inoue: J. Appl. Phys. **99** (2006) 08F102-1–08F102-3.
13) A. Inoue, B. L. Shen, A. V. Yavari and A. L. Greer: J. Mater. Res. **18** (2000) 1487–1492.
14) M. Stoica, J. Eckert, S. Roth, A. R. Yavari and L. Schultz: J. Alloy. Comp. **434–435** (2007) 171–175.
15) A. Inoue, Y. Shinohara and J. S. Gook: Mater. Trans. JIM **36** (1995) 1427–1433.
16) A. Inoue, A. Takeuchi, T. Zhang, A. Murakami and A. Makino: IEEE Trans. Mag. **32** (1996) 4866–4871.
17) T. Zhang and A. Inoue: Mater. Trans. **42** (2001) 1015–1018.
18) D. D. Song, J.-H. Kim, E. Fleury, W. T. Kim and D. H. Kim: J. Alloys Comp. **389** (2005) 159–164.
19) Z. P. Lu, H. Tan, Y. Li and S. C. Ng: Scr. Mater. **42** (2000) 667–673.
20) Z. P. Lu and C. T. Liu: Acta Mater. **50** (2002) 3501–3512.
21) N. S. Naka, M. Mitera and T. Masumoto: Proc. 3rd Intern. Conf. On Rapidly Quenched Metals, Brighton, **2** (1978) pp. 164–171.
22) M. Mitera, M. Naka, T. Masumoto, N. Kazama and K. Watanabe: Phys. Stat. Sol. **(a)49** (1978) K163–K166.
23) M. Naka and T. Masumoto: Sci. Rep. RITU **A27** (1979) 118–126.
24) M. Ohnuma, O. Sasaki, H. Kuwano, S. Katano, Y. Morii, S. Funahashi, H. R. Child and Y. Hamaguchi: Mater. Trans. JIM **34** (1993) 874–881.
25) B. L. Shen and A. Inoue: J. Mater. Sci. Let. **22** (2003) 857–859.